

**WATER-REFLECTED  $^{233}\text{U}$  URANYL NITRATE SOLUTIONS  
IN SIMPLE GEOMETRY**

**Evaluator**

**Karla R. Elam**  
**Oak Ridge National Laboratory\***

**Internal Reviewer**

**Donald E. Mueller**

**Independent Reviewers**

**Richard M. Lell**  
**Roger N. Blomquist**  
**Argonne National Laboratory**

The submitted manuscript has been authored by a contractor of the U.S. Government under contract No. DE-AC05-00OR22725. Accordingly, the U.S. Government retains a nonexclusive, royalty-free license to publish or reproduce the published form of this contribution, or allow others to do so, for U.S. Government purposes.

---

\*Managed by UT-Battelle, LLC, under contract DE-AC05-00OR22725 with the U.S. Department of Energy.

U233-SOL-THERM-005

## WATER-REFLECTED $^{233}\text{U}$ URANYL NITRATE SOLUTIONS IN SIMPLE GEOMETRY

**IDENTIFICATION NUMBER:** U233-SOL-THERM-005

**KEY WORDS:** critical experiment, cylinder, sphere, homogeneous, moderated, water-reflected, solution, thermal,  $^{233}\text{U}$ , uranyl nitrate, acceptable

### 1.0 DETAILED DESCRIPTION

#### 1.1 Overview of Experiment

A number of critical experiments involving  $^{233}\text{U}$  were performed in the Oak Ridge National Laboratory Building 9213 Critical Experiments Facility during the years 1952 and 1953. These experiments, reported in Reference 1, were directed toward determining bounding values for the minimum critical mass, minimum critical volume, and maximum safe pipe size of water-moderated solutions of  $^{233}\text{U}$ . Additional information on the critical experiments was found in the experimental logbooks.<sup>a</sup>

Two experiments utilizing uranyl nitrate ( $\text{UO}_2(\text{NO}_3)_2$ ) solutions in simple geometry are evaluated in this report. Experiment 37 is in a 10.4-inch diameter sphere, and Experiment 39 is in a 10-inch diameter cylinder. The  $^{233}\text{U}$  concentration ranges from 49 to 62 g  $^{233}\text{U}/\text{l}$ . Both experiments were reflected by at least 6 inches of water in all directions.

Paraffin-reflected uranyl nitrate experiments, also reported in Reference 1, are evaluated elsewhere. Experiments with smaller paraffin reflected 5-, 6-, and 7.5-inch diameter cylinders are evaluated in U233-SOL-THERM-004. Experiments with paraffin reflected 8-, 8.5-, 9-, 10-, and 12-inch diameter cylinders are evaluated in U233-SOL-THERM-002. Later experiments with highly-enriched  $^{235}\text{U}$  uranyl fluoride solution in the same 10.4-inch diameter sphere are reported in HEU-SOL-THERM-010.

Both experiments were judged acceptable for use as criticality-safety benchmark experiments.

---

<sup>a</sup> J. K. Fox, Notebook No. Y-NB-1509, Building 9735, September 25, 1951, assigned to C. M. Hopper, Oak Ridge National Laboratory.

J. K. Fox, Notebook No. Y-NB-1859, Building 9213, November 10, 1952, assigned to C. M. Hopper, Oak Ridge National Laboratory.

## **1.2 Description of Experiment Configuration**

Reference 1 describes the reaction vessels as being constructed of 3S aluminum with a Heresite coating to reduce corrosion. The cylindrical vessel was approximately equilateral (a cylinder where the height equals the diameter), based on internal dimensions. Both vessels had attached cylindrical reflector tanks, providing an effectively infinite water reflector in all directions.

Fabrication drawings for similar vessels from the same time period (early 1950's) were located,<sup>a</sup> and it is very likely that the vessels shown in the drawings are the same ones used in this experiment. These drawings indicate that the vessels were fabricated of 16-gage 2S aluminum (0.050821 inches thick according to AWG and B&S gage for non-ferrous sheet).<sup>b</sup> The reflector tanks were made of 1/8" thick 2S aluminum plate. The drawings specify that inner surfaces of the vessels be coated with Heresite.

Reference 1 indicates that there was a safety-blade well attached to the outer surface of the cylindrical vessel, which was designed to accommodate a cadmium blade that could be inserted in event of an excursion. The well was a portion of an annular cylinder which was normally filled with water. According to fabrication drawings, the well was nominally 5/8-inch thick and was constructed of 2S aluminum. For the 10-inch diameter cylinder used in Experiment 39, the safety blade well subtends a 148-degree arc.

The fabrication drawings show a 1-1/4-inch-outside-diameter (OD) tube control-rod well on the outside of the cylindrical reaction vessel that was constructed of 2S aluminum. It is not known whether this well was normally empty or filled with water. The control-rod well had a 2.0-inch-OD X 4-inch-high overflow well at the top. The wall thickness of the control-rod well was approximately 0.040 inch. The inner diameter of the reaction vessel was 10 inches, and the inner height was shown as 9.75 inches. The reaction-vessel bottom was tapered 2 degrees to a 0.5-inch-ID fill/drain pipe located in the center of the bottom. The cylinder was fitted with a 16-gage aluminum cover. The cover was attached to an aluminum flange which was welded to the top of the vessel. The reflector tank inner diameter was shown as 22.125 inches, and the height was 22 inches. The fabrication drawings indicate that the reaction vessel was centered horizontally and vertically within the reflector tank, giving at least six inches of water reflection in all directions. The fill/drain line was connected to the bottom manifold of five rack-mounted, three-inch-diameter stainless-steel pipes which contained the uranyl nitrate solution. The rack was raised and lowered to transfer solution to and from the vessels. The distance between the reaction vessel and the solution manifold is not known. A schematic of the system is shown in Figure 1.

---

<sup>a</sup>Drawings ESK-17285(cylinder) and ESK-17567a (sphere), Oak Ridge Y-12 Plant, Building 9213, 1952.

<sup>b</sup>AWG stands for American Wire Gage, and B&S stands for Brown and Sharpe wire gage. These are both names for the sheet metal gage commonly used in the United States for copper, aluminum, brass, and other non-ferrous alloys. They specify thickness without regard to weight. See O. W. Eshbach, "Handbook of Engineering Fundamentals," Second Edition, John Wiley & Sons, New York, 1952.

The construction of the spherical vessel used in Experiment 37 is not described as thoroughly in Reference 1, and drawing ESK-17567a shows only that the sphere is nominally 10.5 inches in diameter, with 0.050-inch thick walls. HEU-SOL-THERM-010 describes the same vessel, and includes information from one of the later experimentalists (J. T. Thomas). From drawing ESK-17567a and HEU-SOL-THERM-010, the sphere was centered horizontally and supported inside the reflector vessel by two tubes, one used for filling and draining and the other for overflow. The tubes were constructed from the same type of aluminum as the sphere, and were welded to the reflector vessel. J. T. Thomas believes the tubes were 0.25 to 0.5 inches in diameter. The fill/drain tube was connected to the solution manifold like the cylindrical vessel described above. HEU-SOL-THERM-010 shows that the reflector tank was 27.6 inches in diameter and 75.4 inches tall. This configuration provides approximately 8.5 inches of water reflector horizontally, and more than two feet of water reflector vertically around the reaction vessel.

A calibration of volume versus manifold elevation was used to determine the critical volume in the experiments. Appendix B gives a brief description of the methodology used to determine the critical height. For each experiment in a cylindrical vessel, an estimate of the critical volume was made, and the critical height was estimated based on this volume and the calibrated inside area of the tank. The volume in the slightly conical bottom was not included. For the spherical vessels, the experimentalists worked towards achieving a critical configuration with the sphere completely full by adjusting the solution concentration. Because of the uncertainties in the measurement of the solution height/volume, the experimentalist assigned an overall uncertainty of no more than 3% in mass to these experiments (Reference 1).

A neutron source was located in the reflector tank and positioned by remote control. According to Rohrer,<sup>a</sup> the experimental apparatus was positioned inside "Big Sid" (a 9.5-foot-diameter X 10-foot-tall tank located in Building 9213). The boron-lined proportional counter tubes used to monitor the multiplication were located outside of Big Sid. The neutron multiplication was recorded as solution was added incrementally to the reactor tank from the solution manifold, and plots of  $1/M$  vs. solution height were recorded in the logbooks. If the critical state was not achieved, the experiment was extrapolated to critical using this  $1/M$  plot. Reference 1 gives these extrapolated critical parameters with an associated uncertainty.

A photograph of a cylindrical vessel is shown in Figure 2. The reported critical parameters from Reference 1 are given in Table 1.

---

<sup>a</sup> E. R. Rohrer, personal communication to J. T. Shor, July, 1997.

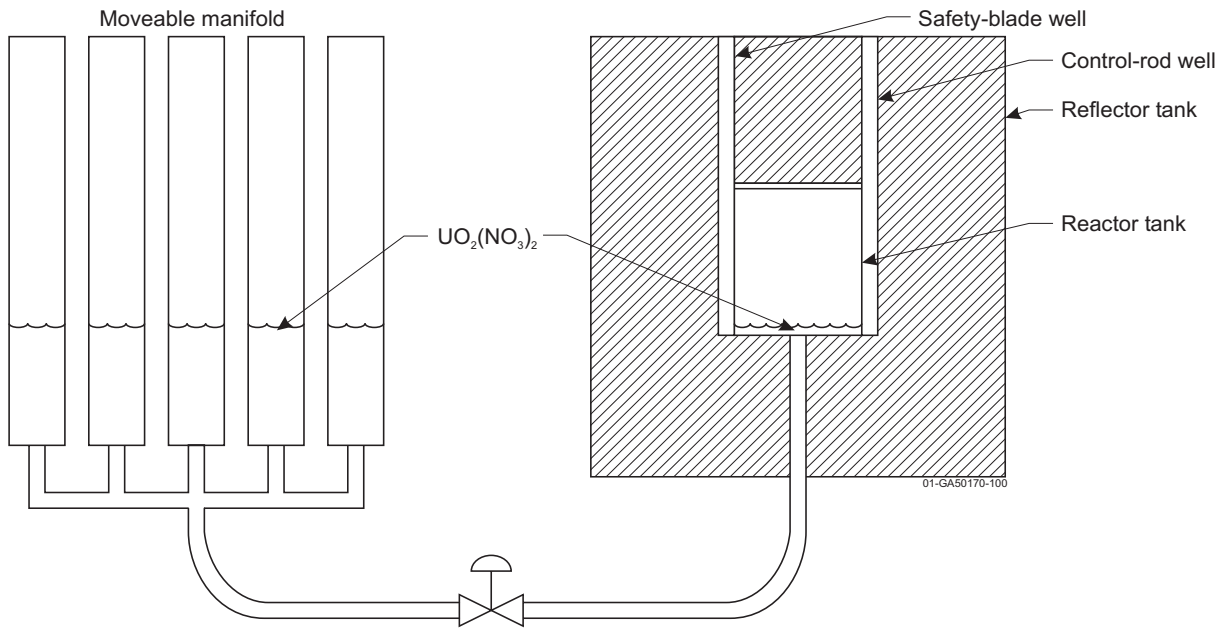


Figure 1. Moveable Manifold.

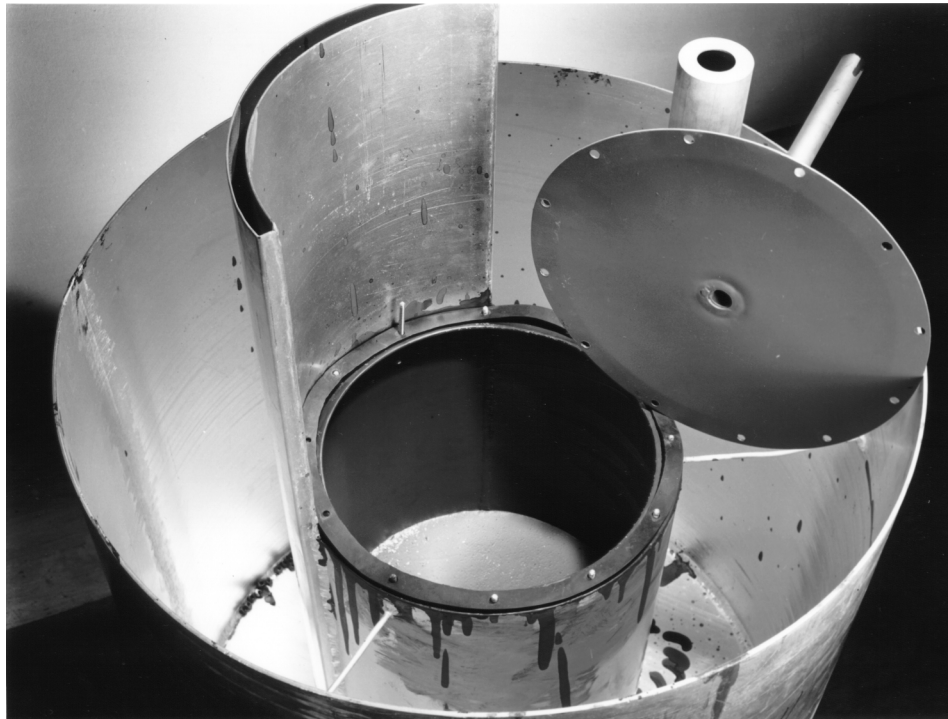


Figure 2. Typical Reaction Vessel.

Table 1. Critical Parameters of Uranyl Nitrate Solutions.

Logbook Experiment #	Diameter (inches)	H/ <sup>233</sup> U	Height (cm)	Volume (liters)	Mass (kg <sup>233</sup> U)
37	10.4 sphere	405	Full	9.66	0.60
39	10.0 cylinder	514	(25.5 ± 0.1) <sup>(a)</sup>	(13.0 ± 0.05) <sup>(a)</sup>	(0.64 ± 0.03) <sup>(a)</sup>

(a) Extrapolated critical parameters.

### 1.3 Description of Material Data

**1.3.1 Solutions** - The isotopic composition of uranium in solution as well as the <sup>233</sup>U concentrations were reported in Reference 1 and are shown in Tables 2 and 3. In Reference 1, the excess acid was reported by stating that the ratio of nitrogen atoms to <sup>233</sup>U atoms (N/<sup>233</sup>U) was 2.66 for all of the reported uranyl nitrate experiments. The principal impurities were also given in Reference 1 and are listed in Table 4. Table 5 lists maximum values for impurities that were tabulated in the logbook but were not reported in Reference 1. Experiment notes in the logbooks indicate that total nitrate was measured and excess nitrate was calculated based on total nitrates and uranium concentration. Therefore, the excess acid includes the nitrates associated with the impurities that form nitrate compounds. Reference 1 does not report any specific uncertainties associated with solution measurements.

From the logbooks, we know that the uranium was received at Building 9213 in 10 small solution batches ranging in uranium mass from about 60 grams to 350 grams per batch. The <sup>233</sup>U purity ranged from 97.65% to 99.06%. The <sup>232</sup>U impurity in the solutions was less than 4x10<sup>-4</sup> wt.% of U.

Table 2. Isotopic Composition of Uranium in Solution (Reference 1).

Isotope	Wt. %
<sup>233</sup> U	98.7
<sup>234</sup> U	0.50
<sup>235</sup> U	0.01
<sup>238</sup> U	0.79

Table 3. <sup>233</sup>U Concentration in Solutions (Reference 1).

Logbook Experiment #	H/ <sup>233</sup> U Atomic Ratio	Solution Density (g/cm <sup>3</sup> )	g <sup>233</sup> U per g of Solution	g <sup>233</sup> U per cm <sup>3</sup> in Solution
37 (sphere)	405	1.087	0.057	0.062
39 (cylinder)	514	1.069	0.046	0.049

Table 4. Principal Impurities in Solution (Reference 1).

Element	Before use (ppm) <sup>(a)</sup>	After use (ppm)
Al	15	50
Ca	300	1500
Cr	10	15
Fe	20	300
Mg	10	125
Ni	20	70
Th	150	(Not given)

(a) The convention for the ppm impurity specification was not given, but it appears from the logbook that the analysis was for the solution such that ppm refers to ppm of solution by weight.

Table 5. Additional Impurities Not Originally Reported (logbook Y-NB-1509).

Element	Maximum (ppm)
B	17
Cu	16.8
Mn	16.2
Pb	97.7
Ti	9.77

The excess acid was not measured for each experimental solution. It appears that two measurements of excess acid were made during this entire series of uranyl nitrate experiments. The experimentalist used the measured specific gravity, uranium content (g U/g), and excess acid to estimate the water density in the solution and to calculate the H/<sup>233</sup>U.

Table 6 gives the solution parameters from logbook Y-NB-1859. These values contain more significant figures than those reported in Reference 1.

Table 6. Measured Solution Parameters (logbook Y-NB-1859).

Logbook Experiment #	Date (Year = 1952)	H/X	Sample Temp (°C)	Solution Density (g/cc)	g U per g of Solution
37	11/20-21	405	27	1.0875	0.05820
39	11/26	514	26.2	1.0686	0.04675

**1.3.2 Non-Fissile Materials** - Reference 1 indicates that the vessels were fabricated from 3S aluminum coated with a thin layer of Heresite. However, as described in Section 1.2, fabrication drawings for similar vessels made during the same time period indicate that the vessels were typically fabricated from 2S aluminum with all inside surfaces coated with Heresite. HEU-SOL-THERM-010 describes the spherical vessel used in Experiment 37, and indicates it is made of 2S aluminum. Table 7 shows the compositions of 2S and 3S aluminum.

The composition of Heresite is not reported. However, a representative<sup>a</sup> of the Heresite Protective Coatings Company suggests that Heresite is a compound containing phenolic resin with iron oxide. The mixture was not known but it was suggested that the coating be 10:1 phenol-to-iron oxide molecules, giving a formula for Heresite of  $(C_6H_5OH)_{10}(FeO)$ .

Table 7. Compositions of 2S and 3S Aluminum.  
(from ASME Metals Handbook, 1954)

Element	2S weight % <sup>(a)</sup>	3S weight % <sup>(a)</sup>
Al	99.0	97.2
Si	1.0	0.6
Mn	0.1	1.2
Cu	0.2	0.2
Zn	0.03	0.1

(a) Impurity weight percents are maximum values.

#### 1.4 Supplemental Experimental Measurements

No supplemental experimental measurements were recorded for this set of experiments.

---

<sup>a</sup> Heresite is made by the Heresite Protective Coatings Co. in Manitowoc, WI. This company was founded in 1935 and patented Heresite in 1937. A company representative, Jerry Treuttner, suggested that the coating was probably P-403, Baking Phenolic Coating. He stated that once the phenolic coating is fully bake-cured, a thin coating of phenolic polymer and iron oxide pigments is left. Other organic compounds are removed during the curing process.



## 2.0 EVALUATION OF EXPERIMENTAL DATA

The experimentalists report that the  $^{233}\text{U}$  masses from critical experiments with uranyl nitrate in Heresite-lined vessels had an uncertainty of no more than  $\pm 3\%$ . They indicated that a large portion of this uncertainty is due to the indirect method of solution height measurement used for the uranyl nitrate experiments.

The experimental uncertainties will be evaluated by two methods. First the uncertainties will be estimated based on applying reasonable uncertainties on each of the experimental parameters that affect criticality for these systems. The uncertainty estimated by this method will then be compared to the uncertainty that would result from applying the experimentalists' stated maximum uncertainties in  $^{233}\text{U}$  critical mass.

### 2.1 Solution Uncertainties

The uranyl nitrate solution used in the experiments described in U233-SOL-THERM-002 and U233-SOL-THERM-004 was also used for the experiments described here.

Two groups of uncertainties and approximations related to the solution are evaluated here. These are 1) uncertainties in isotopic composition, 2) uncertainties in solution composition, including uranium concentration, density, excess acid, and impurities. To avoid the statistical uncertainties of Monte Carlo codes, the XSDRNPM discrete-ordinates code was used along with the SCALE 238-group ENDF/B-V cross section library to evaluate solution uncertainties. The geometry was taken as a sphere or a buckled cylinder with an aluminum wall and six inches of radial water reflection. The overall convergence criteria and point convergence criteria were set to  $1\text{E-}5$ , and the order of angular quadrature was  $S_8$ .

**2.1.1 Isotopic Composition** - As noted above, the uranyl nitrate solution used in the experiments described in U233-SOL-THERM-002 and U233-SOL-THERM-004 was used for the experiments in this evaluation, and so should contain the same isotopic composition. In Section 2.1.1 of U233-SOL-THERM-002, the method used to prepare the uranyl nitrate solution is described, along with an analysis of the reported isotopic composition compared to logbook data. It was concluded that the  $^{233}\text{U}$  isotopic content should be 98.66 wt % based on the logbook data. The  $^{234}\text{U}$  and  $^{238}\text{U}$  contents were determined to be 0.46 wt % for the  $^{234}\text{U}$  content and 0.88 wt % for the  $^{238}\text{U}$  content. (These values may be compared to the isotopic content reported in Reference 1 of 98.7 wt %  $^{233}\text{U}$ , 0.50 wt %  $^{234}\text{U}$ , 0.01 wt %  $^{235}\text{U}$ , and 0.79 wt %  $^{238}\text{U}$ .)

The isotopic composition and associated uncertainties from U233-SOL-THERM-002 were taken as the reference values for this evaluation. The  $^{234}\text{U}$  content was taken as  $0.46 \pm 0.10$  wt % and the  $^{238}\text{U}$  content was taken as  $0.88 \pm 0.20$  wt %. The  $^{233}\text{U}$  content was determined by difference. For this sensitivity analysis, each minor uranium isotope was varied separately, with  $^{233}\text{U}$  being varied simultaneously to keep the total uranium content constant. The results of the sensitivity analysis are shown in Table 8. These uncertainties were assigned a confidence level of one  $\sigma$ , and as can be seen from Table 8, their contribution to the overall benchmark uncertainty is small.

Also evaluated was the change in calculated  $k_{eff}$  from using the reference enrichment values relative to the isotopic composition reported in Reference 1. For experiment 37, the  $\Delta k_{eff} = 0.000005$ , and for experiment 39,  $\Delta k_{eff} = -0.000010$ . These values are smaller than those shown in Table 8 for uncertainties due to possible variations in  $^{234}\text{U}$  and  $^{238}\text{U}$  content, so those in Table 8 will be used in determining the uncertainty due to isotope composition.

Table 8. Effects of Solution Uncertainties.

Parameter	Variation	Experiment 37 $\Delta k_{eff}$	Experiment 39 $\Delta k_{eff}$
$^{234}\text{U}$ wt %	$\pm 0.1$ wt % <sup>(a)</sup>	$\mp 0.00043$	$\mp 0.00046$
$^{238}\text{U}$ wt %	$\pm 0.2$ wt % <sup>(a)</sup>	$\mp 0.00057$	$\mp 0.00063$
excess acid	$\pm 10\%$	$\mp 0.00051$	$\mp 0.00042$
density	$\pm 0.3\%$	$\pm 0.00150$	$\pm 0.00143$
g U/g solution	$\pm 0.5\%$ $(\pm 3.0\%)^{(b)}$	$\pm 0.00100$ $(\pm 0.00616)^{(b)}$	$\pm 0.00124$ $(\pm 0.00766)^{(b)}$
impurities	+ maximum impurities	- 0.00348 <sup>(c)</sup>	- 0.00416 <sup>(c)</sup>

<sup>a</sup> The total uranium content was kept constant by varying the  $^{233}\text{U}$  wt % with the parameter shown.

<sup>b</sup> Not included in total uncertainty. See Section 2.3.

<sup>c</sup>  $\Delta k_{eff}$  adjusted from  $3\sigma$  confidence level to  $1\sigma$  confidence level.

**2.1.2 Solution Composition** - The logbook provides some of the details of the solutions used in these experiments. The solution specific gravity and uranium concentration in g U/g solution were specified for each experiment. The excess acid was measured for only two solutions. Also provided was the temperature of the solution samples at the time they were analyzed in the laboratory. The data from the logbook are presented in Table 6.

The excess-acid content has the largest individual uncertainty of the three solution parameters. Review of the logbooks indicates that it was measured directly for only two of the solutions in the entire series of 39 uranyl nitrate experiments. The first measurement was at the beginning of the series, and the second measurement was after the solution had been adjusted near the midpoint of the series. Reference 1 simply indicates that the  $\text{N}/^{233}\text{U}$  ratio was constant at 2.66 for all of the uranyl nitrate solutions. It was therefore assumed that the excess acid to  $^{233}\text{U}$  concentration remained fairly constant throughout the subsequent dilutions. The two experiments evaluated here fell into the last half of the total series of experiments. The logbook reports that the excess acid was 0.0352 g  $\text{HNO}_3/\text{g}$  at experiment 20, and Reference 1 gives a concentration of 0.197 g  $^{233}\text{U}/\text{g}$  for that solution. (Note that if these values are used to calculate number densities for the solution at experiment 20, the  $\text{N}/^{233}\text{U}$  ratio is actually 2.69.) By maintaining proportionality between reported uranium

concentration and excess acid concentration, the excess acid for experiment 37 is 0.0102 g HNO<sub>3</sub>/g, and for experiment 39, it is 0.00822 g HNO<sub>3</sub>/g. The excess acid is a small constituent in the solution; however, since an additive relationship is used to determine the water content, any uncertainty in the excess acid translates into an uncertainty in H/<sup>233</sup>U. The assumed uncertainty in excess acid for each experiment was taken as ±10%, with a confidence level of one  $\sigma$ . While the excess acid concentration was varied, the solution density and uranium density were held constant. The results of this uncertainty in the excess-acid content are presented in Table 8.

In Reference 1, the solution densities were reported to three decimal places for all experiments, which implies that there was only a small uncertainty in the measurement ( $\pm 0.0005$  g/cm<sup>3</sup>). However, the terms "specific gravity" and "density" were used interchangeably in the logbook and in Reference 1. The difference in specific gravity and density is related to the temperature and density of water used as a standard. The specific gravity is the ratio of solution density to water density at a given temperature, whereas the density is the actual density of the solution. Temperatures are reported for the laboratory samples in the logbook. These varied from 26.2°C to 27°C. Over this temperature range, the density of water ranges from 0.9967 to 0.9965. Therefore, if the solution specific gravity is measured but the value is reported as a density, the difference would be approximately 0.3%. Since it is not known which parameter was actually measured for these solutions, an uncertainty of  $\pm 0.3\%$  is applied to the density, with a confidence level of one  $\sigma$ . The uncertainty associated with the density measurement itself,  $\pm 0.05\%$ , is small compared to this  $\pm 0.3\%$  uncertainty, and so will be neglected. While the solution density was varied, the uranium density and excess acid density were held constant, thus giving an indication in the uncertainty associated with water concentration. The results are presented in Table 8.

Reference 1 estimates that there is an uncertainty of  $\pm 0.5\%$  associated with the uranium analysis, and it is assumed that this corresponds to a one  $\sigma$  confidence level. This uncertainty may be evaluated by performing a  $\pm 0.5\%$  variation on the uranium concentration. The results of this calculation are presented in Table 8. While the uranium concentration was varied, the solution density and excess acid density were held constant. Also given in Table 8 are the variations associated with a  $\pm 3.0\%$  variation in uranium concentration or critical mass. This is the maximum overall uncertainty reported by the experimenters for these experiments, and will be discussed further in Section 2.3.

The impurities in the solution were given in Reference 1 and in logbook Y-NB-1509, and are repeated in Tables 4 and 5 of this evaluation. Data for the impurities given in Table 4 are given as before and after use of the solution, which is assumed to mean the beginning and the end of the series of 39 experiments utilizing this uranyl nitrate solution. Since the two experiments evaluated here were performed at the end of this series, it is reasonable to assume that the "after use" impurity levels from Table 4 would have been present. However, this is not known accurately enough to be considered a bias in the benchmark model. The impurities listed in Table 5 were not reported in Reference 1, and it is not known when the sample for this analysis was taken. The magnitude of the effect of the impurities was evaluated based on calculations with and without the maximum level of

each impurity, and this uncertainty was assigned a three  $\sigma$  confidence level.<sup>a</sup> No attempt was made to adjust the nitrate content of the solution due to the presence of the impurities, many of which form nitrate compounds in such a solution. The variability applied to the excess acid should easily bound the effects of any additional nitrate that could have been present. After adjusting the uncertainty to a one  $\sigma$  confidence level, the effect of adding the impurities is given in Table 8.

## 2.2 Geometry Uncertainties

The geometry uncertainties considered in this evaluation are uncertainties in the solution height for Experiment 37, the radius of the vessels, the wall thickness, and the effect of the Heresite liner. All of the geometry uncertainty calculations, except for the solution height and Heresite liner for Experiment 37, were performed using the XSDRNPM discrete-ordinates code with the SCALE 238-group ENDF/B-V cross-section library. The geometry was taken as a sphere or a buckled water-reflected cylinder with an aluminum wall. The overall convergence criteria and point convergence criteria were set to 1E-5, and the order of angular quadrature was  $S_8$ . The sensitivities for the solution height and Heresite liner for Experiment 37 were performed using SCALE 4.4 KENO V.a and the SCALE 238-group ENDF/B-V cross-section library, with enough neutron histories to produce a maximum Monte Carlo  $\sigma$  of 0.0003. The geometry used was the simplified 3-D model which is described in Section 3. The maximum  $\Delta k_{eff}$  obtained between the base case and the perturbed case is reported as the uncertainty.

**2.2.1 Solution Height** - The measurement of solution height is usually a significant factor in the geometry uncertainty for this type of experiment. However, for the two experiments evaluated here, the endpoint was a completely full vessel. Experiment 37 in the sphere was critical completely full, and in Experiment 39, the full cylinder was slightly subcritical and the "true" critical height was determined by extrapolation of the source neutron multiplication data.

Notes in the logbook of critical-height data indicated that the height of the fissile solution in the vessel was measured indirectly using a combination of calibrated volumes and the measured elevation of the solution manifold. Solution was introduced into the vessels by moving the manifold that was attached as shown in Figure 1. The zero for the height measurement for each system was slightly different and the experimenters estimated a dead volume that was added (or subtracted) from the volume due to the change in elevation of the storage rack. It appeared that the dead volume was adjusted for the small volume of the cone-shaped bottom of the cylinder in Experiment 39 such that the reported height was that of only the solution in the straight portion of the cylinder. The height of a cylinder with a volume equivalent to the conical bottom must be added to the measured solution height to compensate for replacing the conical bottom with a flat bottom cylinder in computer models. For this 10-inch cylinder, this equivalent height is 0.1482 cm.

---

<sup>a</sup>In a separate set of calculations, the boron impurity was evaluated separately. It was determined that the boron impurity accounts for nearly 97% of the total impurity uncertainty.

Since the sphere in Experiment 37 was critical completely full, no solution height uncertainty will be associated with that experiment. However, Experiment 39 was extrapolated from a measured height of 25.1 cm to a reported critical height of  $25.5 \pm 0.1$  cm. Therefore, an experimental uncertainty of  $\pm 0.1$  cm in solution height has been applied to Experiment 39, and the result is shown in Table 9. Reference 1 does not give the confidence level associated with the  $\pm 0.1$  cm. Examination of the logbook indicates that the uncertainty is not associated with reproducibility of the critical extrapolation, since this configuration was only taken on one approach to critical. It appears that the uncertainty is the experimenter's best guess at the uncertainty on the extrapolation, and so it is assigned a one  $\sigma$  confidence level.

**2.2.2 Vessel Radius** - Drawings that were located for vessels made during the same time period indicate that the allowed uncertainty in the dimensions for non-machined surfaces ranges from  $\pm 1/64$  inch to  $\pm 1/32$  inch. The radius for each vessel was determined by the experimentalists by a volume calibration in which the increase in height was measured for incremental volume additions.

The volumetric calibration for the 10.4-inch sphere was found in a logbook. Two different calibrations are shown, one using 200 mL additions, and one using 1 liter additions. The first calibration resulted in a volume of 9.670 liters, and the second one gave 9.645 liters. The experimentalist noted in the logbook that he believed the second calibration was more accurate. However, in Reference 1, the volume is given as 9.66 liters, which is approximately the average of the two calibration values. (Subsequent experiments using this vessel, reported in HEU-SOL-THERM-010, gave a volume of 9.661 liters at 27.5°C.) Converting the two calibration volumes to a radius yields 13.2050 cm for a volume of 9.645 liters, and 13.2163 cm for a volume of 9.670 liters.

The published volume given in Reference 1, 9.66 liters, will be used to calculate the inner radius of the sphere for this evaluation, which is 13.2118 cm. Based on the calibration data, the uncertainty in the inner radius will be calculated using an uncertainty in the volume of  $\pm 0.01$  liters, giving an uncertainty in inner vessel radius of  $\pm 0.0045$  cm. The thicknesses of the vessel wall and the reflector remained constant for these calculations. A one  $\sigma$  confidence level was assigned to this uncertainty, and its contribution to the overall experimental uncertainty is small. The result is shown in Table 9.

No volumetric calibration for the 10-inch diameter cylinder could be found in the logbooks, but the calibrated inner area is given as 509 cm<sup>2</sup>, giving a radius of 12.7287 cm. Based on this calibration data, the uncertainty in the internal area will be calculated using  $\pm 1$  cm<sup>2</sup>, giving an uncertainty in inner vessel radius of  $\pm 0.02$  cm. The thicknesses of the vessel wall and the reflector remained constant for these calculations. Again, a one  $\sigma$  confidence level was assigned to this uncertainty, and its contribution to the overall experimental uncertainty is small. The result is shown in Table 9.

**2.2.3 Wall Thickness** - The wall of each vessel was manufactured of 16-gage type-2S aluminumplate. The density of 2S aluminum is taken as 2.71 g/cm<sup>3</sup> in this evaluation.<sup>a</sup> The nominal

---

<sup>a</sup> Handbook of Chemistry and Physics, 40<sup>th</sup> Edition, 1958-1959.

thickness of 16-gage aluminum is 0.05081 in. (0.1291 cm).<sup>b</sup> Drawings of similar vessels constructed during the same time frame give the wall thickness as 0.050 inches. The wall thickness was varied by the standard mill tolerance of  $\pm 12\text{-}1/2\%$  (0.0161 cm)<sup>a</sup> to bound the uncertainties in using the nominal gage thickness in the model while holding the inside solution radius and the reflector thickness constant. Because this uncertainty is derived from a mill tolerance value, it is assigned a three  $\sigma$  confidence level. After adjusting the uncertainty in  $k_{eff}$  to a one  $\sigma$  level, the results are presented in Table 9.

**2.2.4 Heresite Liner** - Heresite was used to coat the inside surfaces of these vessels. The thickness of the Heresite liner was not reported. It was estimated to be 0.061 cm thick in U233-SOL-THERM-004 for a similar 6-inch-diameter cylindrical vessel, and 0.0254 cm (10 mils) thick in HEU-SOL-THERM-010 for the same 10.4-inch diameter sphere. A fabrication drawing for a spherical reaction vessel which dates from 1957 specifies a Heresite lining of 0.030 inches, or 0.0762 cm, thick.

HEU-SOL-THERM-010 described the composition of Heresite as mixture of phenol and iron oxide with a molecular ratio of 10:1. Using a density of 1.072 g/cm<sup>3</sup> for the phenol and 5.7 g/cm<sup>3</sup> for the FeO, and assuming volume additivity, the combined density of the Heresite is 1.138 g/cm<sup>3</sup>.

To evaluate the uncertainty due to the unknown thickness and composition of the Heresite liner, calculations were performed both with and without a Heresite layer that was 0.0762 cm thick, and with a density of 1.138 g/cm<sup>3</sup>. The solution radius remained the same, as did the thickness of the aluminum wall and the thickness of the reflector. The calculations for Experiment 39 were performed using KENO V.a so that the Heresite liner could be placed on the top and bottom of the cylinder, as well as around the sides. Results of these calculations are given in Table 9. Since the actual thickness and composition of the Heresite liner are unknown, and since the reactivity change is small, this will be treated as an uncertainty. However, since it was evaluated using the maximum reported thickness, the calculated uncertainty has been adjusted from a three  $\sigma$  confidence level to a one  $\sigma$  confidence level.

Table 9. Effects of Geometry Uncertainties.

Parameter	Variation	Experiment 37 $\Delta k_{eff}$	Experiment 39 $\Delta k_{eff}$
Solution height	$\pm 0.1$ cm	N/A	$\pm 0.0011$
Vessel radius	$\pm 0.0045$ cm	$\pm 0.00026$	—
	$\pm 0.02$ cm	—	$\pm 0.00078$
Wall thickness	$\pm 0.0161$ cm	$\mp 0.00011^{(a)}$	$\mp 0.00025^{(a)}$
Heresite liner	0.0762 cm liner removed	$- 0.00012^{(a)}$	$- 0.00023^{(a)}$

<sup>b</sup> Marks' Standard Handbook for Mechanical Engineers, 8<sup>th</sup> Edition, 1978.

<sup>a</sup>  $\Delta k_{eff}$  adjusted from 3 $\sigma$  confidence level to 1 $\sigma$  confidence level.

### 2.3 Combination of Uncertainties

The overall uncertainties assigned to these two benchmarks are given by a combination of the uncertainties given in Tables 8 and 9. Combined uncertainties are determined by taking the square root of the sum of the squares for all included one  $\sigma$  confidence level uncertainties, and are given in Table 10. For Experiment 37, this combined uncertainty in  $k_{eff}$  is  $\pm 0.0040$ , and for Experiment 39, it is  $\pm 0.0049$ . These overall uncertainties are sufficiently small to qualify these experiments as acceptable benchmarks.

Table 8 gives the uncertainty in  $k_{eff}$  associated with a 3% variation in uranium concentration or critical mass. In Reference 1, the experimentalists gave an uncertainty of "no more than  $\pm 3\%$ " for these critical mass measurements with uranyl nitrate in Heresite-lined vessels. The uncertainties in  $k_{eff}$  given in Table 8 for a 3 % change in uranium mass (uranium concentration - gU/g) are 0.00616 for experiment 37 and 0.00766 for experiment 39. These bound the uncertainties determined for the benchmarks, and so the benchmark uncertainties are consistent with the value given by the experimentalists.

Table 10. Combined Uncertainties

Parameter	Experiment 37 $\Delta k_{eff}$	Experiment 39 $\Delta k_{eff}$
<sup>234</sup> U wt %	$\mp 0.00043$	$\mp 0.00046$
<sup>238</sup> U wt %	$\mp 0.00057$	$\mp 0.00063$
excess acid	$\mp 0.00051$	$\mp 0.00042$
density	$\pm 0.00150$	$\pm 0.00143$
g U/g solution	$\pm 0.00100$	$\pm 0.00124$
impurities	- 0.00348	- 0.00416
Solution height	N/A	$\pm 0.0011$
Vessel radius	$\pm 0.00026$	$\pm 0.00078$
Wall thickness	$\mp 0.00011$	$\mp 0.00025$
Heresite liner	- 0.00012	- 0.00023
Combined uncertainty	$\pm 0.0040$	$\pm 0.0049$

### 3.0 BENCHMARK SPECIFICATIONS

#### 3.1 Description of Model

**3.1.1 Case 1 (Experiment 37)** - A detailed model of the sphere used in experiment 37 (benchmark case 1) was developed that included the fill/drain and overflow tubes and the cylindrical reflector tank walls, using reflector and tube dimensions from HEU-SOL-THERM-010, Figure 2. The reflector tank had a inner radius of 35 cm, giving a minimum of 21.66 cm (8.53 in) of water reflection. The tubes had an inner diameter of 1.016 cm (0.4 in). The fill/drain tube was filled with solution, and the overflow tube was filled with void. This was compared to a simplified model containing only the spherical reactor tank, including the aluminum walls, with a uniform 15.24 cm (6 inches) water reflector on all sides. KENO V.a and the SCALE 238-group ENDF/B-V cross-section library were used for the comparison, with sufficient histories to obtain a  $\sigma$  of 0.0005. The  $\Delta k_{eff}$  for this simplification is 0.0003, which is less than the Monte Carlo standard deviation of 0.0005. Therefore, no bias will be associated with this model simplification.

**3.1.2 Case 2 (Experiment 39)** - The actual experimental set up for the cylinder used in experiment 39 (benchmark case 2) has many more complicating factors. The set up included safety blade and control rod wells and an overflow well, in addition to a fill/drain tube and a reflector tank. Also, the bottom of the reactor tank was not flat, but had a slight conical shape. In U233-SOL-THERM-004, full detailed models were developed to evaluate modeling simplifications for similar experiments in cylindrical vessels. (These experiments were paraffin-reflected, but had the safety blade guide region filled with water.) It was determined that the replacement of the water filled safety blade guide with paraffin had the largest effect when simplifying the geometry model. The one cylindrical experiment evaluated here used water reflection, so the only effect of this simplification is to eliminate the safety blade guide aluminum wall. The simplification with the next largest bias in U233-SOL-THERM-004 was the elimination of the Heresite liner, which was discussed as an uncertainty in Section 2.2.4 of this evaluation. Other model simplifications, such as omitting the fill/drain line and replacing the conical bottom with an equivalent volume flat bottom, had negligible effects on the value of  $k_{eff}$  in U233-SOL-THERM-004, and have not been evaluated separately in this report.

A detailed model for case 2 that included only the water-filled safety blade guide and the reflector with 1/8-inch thick aluminum reflector tank was developed. This model was used to determine any bias for the simplified model in which the safety blade guide was omitted and a uniform water reflector thickness of 15.24 cm (6 inches) was considered on all faces. KENO V.a and the SCALE 238-group ENDF/B-V cross-section library were used for the comparison, with sufficient histories to obtain a Monte Carlo  $\sigma$  of 0.0003. The  $\Delta k_{eff}$  for this simplification is 0.0002, which is less than the Monte Carlo standard deviation of 0.0003. Therefore, no bias will be associated with this model simplification.

**3.1.3 Room Return and Solution Impurities** - Room return has been neglected for these experiments. Effects of room return, or return of neutrons from nearby equipment and structures, is



insignificant for faces reflected with 6 inches of water. Solution impurities are not well known, and are therefore omitted from the benchmark models. This is evaluated as an uncertainty in Section 2.1.2.

### 3.2 Dimensions

The simplified benchmark model for Case 1 (Experiment 37) is a sphere of solution with a radius of 13.2118 cm, surrounded by an aluminum wall that is 0.1291 cm thick and a 15.24 cm thick water reflector. This gives three concentric spheres with radii of 13.2118 cm, 13.3409 cm, and 28.5809 cm, respectively. This model is shown in Figure 3.

The simplified benchmark model for Case 2 (Experiment 39) is a right circular cylinder of solution with a radius of 12.7287 cm, as shown in Figure 4. The inner height of the cylinder is 25.6482 cm, which includes the reported solution height of 25.5 cm, and the height associated with the equivalent volume of the conical bottom, which is 0.1482 cm. This solution cylinder is surrounded on all sides by 0.1291 cm of aluminum, and then by 15.24 cm of water reflector.

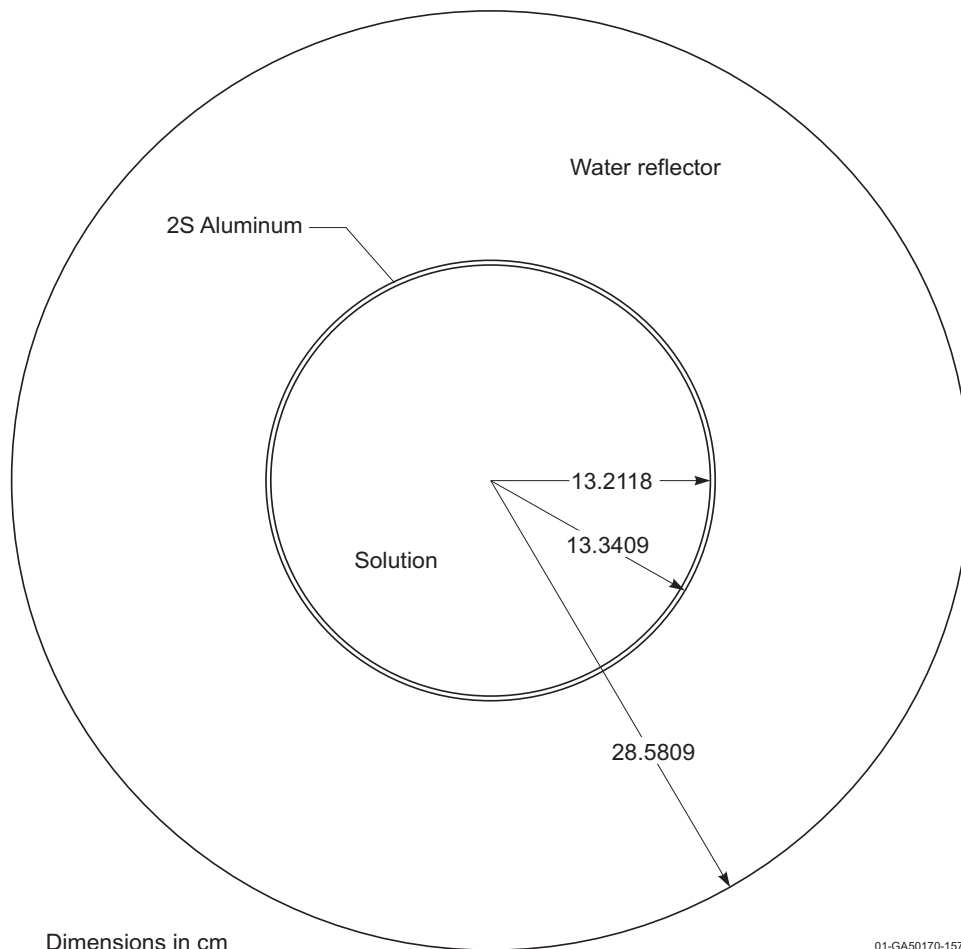


Figure 3. Benchmark Model of Case 1 (sphere).

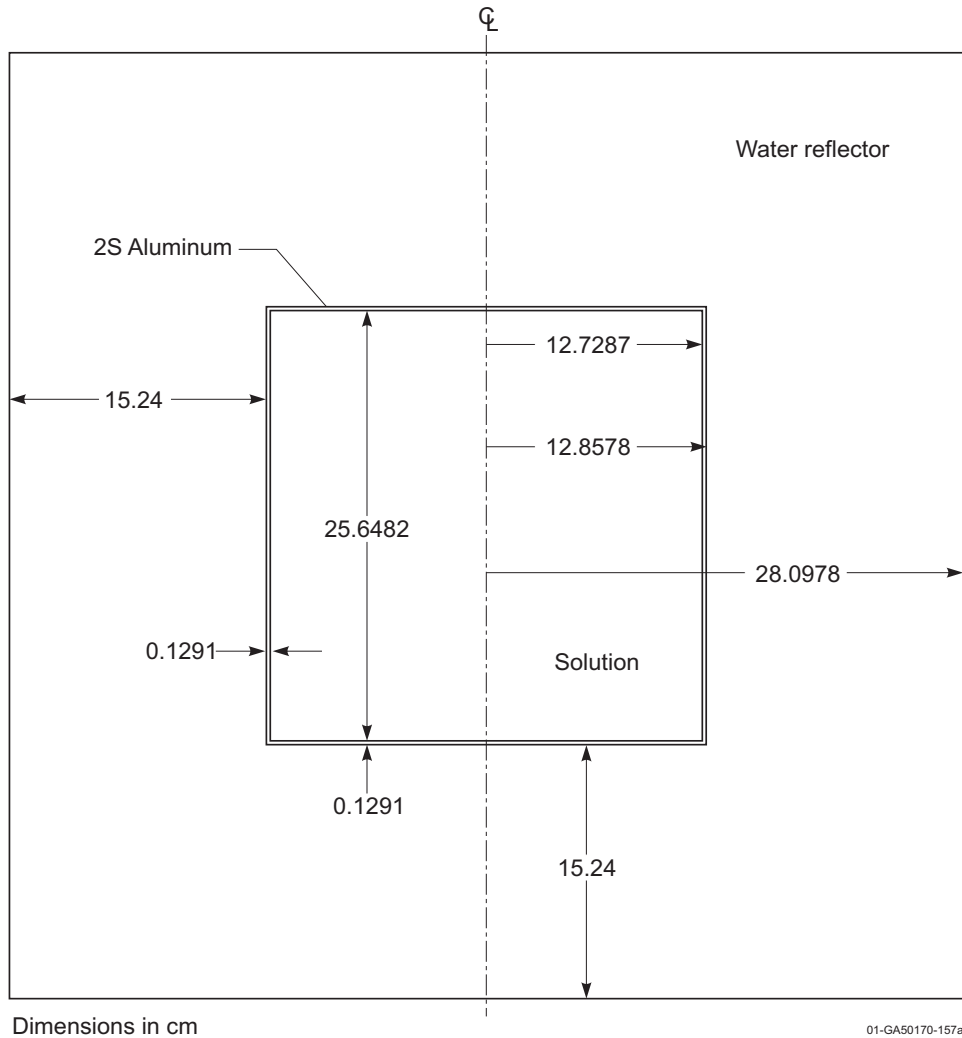


Figure 4. Benchmark Model for Case 2 (cylinder).

### 3.3 Material Data

Table 11 contains the atomic number densities for the fissile solution determined from the data in Table 3 and using the isotopic distribution derived in Section 2.1.1 and the excess acid concentrations derived in Section 2.1.2. The atom densities are shown as atoms per barn-centimeter. Atom densities were calculated using the following formulas (where 0.9866 is the weight fraction of  $^{233}\text{U}$  in uranium):

$$\frac{gU}{g_{solution}} = \frac{g^{233}U}{0.9866}$$

$$\rho_U = \rho_{solution} \times \frac{gU}{g_{solution}}$$

$$\rho_{HNO_3} = \rho_{solution} \times \frac{gHNO_3}{g_{solution}}$$

$$\rho_{UO_2(NO_3)_2} = \rho_U \times \frac{M_{w,UO_2(NO_3)_2}}{A_{w,U}}$$

$$\rho_{H_2O} = \rho_{solution} - \rho_{UO_2(NO_3)_2} - \rho_{HNO_3}$$

$$N_{H_2O} = N_A \times \frac{\rho_{H_2O}}{M_{w,H_2O}}$$

$$N_{HNO_3} = N_A \times \frac{\rho_{HNO_3}}{M_{w,HNO_3}}$$

$$\rho_{^{233}U} = \rho_{solution} \times \frac{g^{233}U}{g_{solution}}$$

$$\rho_{^{234}U} = \rho_{^{233}U} \times \frac{0.0046}{0.9866}$$

$$\rho_{^{238}U} = \rho_{^{233}U} \times \frac{0.0088}{0.9866}$$

$$N_{U_i} = N_A \times \frac{\rho_{U_i}}{A_{w,U_i}}$$

$$N_U = \sum_i N_{U_i}$$

$$N_H = N_{HNO_3} + (2 \times N_{H_2O})$$

$$N_O = (3 \times N_{HNO_3}) + N_{H_2O} + (8 \times N_U)$$

$$N_N = N_{HNO_3} + (2 \times N_U)$$

Table 11. Atomic Number Densities for the Experimental Solutions.

Case	$^{233}\text{U}$	$^{234}\text{U}$	$^{238}\text{U}$	H	O	N
1	1.6011E-04	7.4332E-07	1.3981E-06	6.5028E-02	3.4077E-02	4.3047E-04
2	1.2707E-04	5.8994E-07	1.1096E-06	6.5403E-02	3.3942E-02	3.4152E-04

Table 12 shows the atom densities for 2S aluminum. Only the aluminum and silicon components were included in the aluminum specification. A density of 2.71 g/cm<sup>3</sup> was used.

Table 12. Atom Number Densities for  
2S Aluminum.

Component	Atom Density
Al	5.9881E-02
Si	5.8108E-04

Table 13 gives the atom densities used for the water reflector. A density of 0.9982 g/cm<sup>3</sup> was used, which corresponds to a temperature of 293 K.

Table 13. Atom Number Densities for  
Water Reflector.

Component	Atom Density
H	6.6735E-02
O	3.3368E-02

### 3.4 Temperature Data

No solution temperatures were given for the experiments. All temperatures for the benchmarks model were taken as 293 K.

### 3.5 Experimental and Benchmark-Model $k_{eff}$

The experimental  $k_{eff}$  for both of the experiments is taken as  $k_{eff} = 1.0000$ . There is no bias associated with the model simplifications discussed in Section 3.1, so the benchmark  $k_{eff}$  is also 1.0000. The

experimental uncertainties were summarized in Section 2.3, making the simplified benchmark model  $k_{eff}$  for Case 1 equal to  $1.0000 \pm 0.0040$  and for Case 2 equal to  $1.0000 \pm 0.0049$ .

#### 4.0 RESULTS OF SAMPLE CALCULATIONS

Results for  $k_{eff}$  are given in Table 14. Input listings for each code are given in Appendix A. Each result was found using the simplified model as described in Section 3.2 and the atom densities defined in Section 3.3.

The results using the SCALE 27-group ENDF/B-IV library over-predict  $k_{eff}$  by as much as 1.3%. The calculations using the ENDF/B-V cross section libraries are in better agreement with the benchmark-model  $k_{eff}$ . Hydrogen with a water thermal kernel was utilized for both the MCNP4C and KENO V.a calculations using the ENDF/B-V libraries.

Table 14.a. Sample Calculation Results (United States).

Code (Cross Section Set→ Case #↓	KENO V.a (27-Group ENDF/B-IV)	KENO V.a (238-Group ENDF/B-V)	MCNP4C (Continuous Energy ENDF/B-V.0)	VIM (Continuous Energy ENDF/B-V.0) <sup>a</sup>	VIM (Continuous Energy ENDF/B-VI.3) <sup>a</sup>
1	1.0132 ± 0.0021	0.9988 ± 0.0023	1.0048 ± 0.0017	1.0051 ± 0.0009	1.0004 ± 0.0009
2	1.0119 ± 0.0023	0.9991 ± 0.0020	1.0060 ± 0.0016	1.0089 ± 0.0010	1.0027 ± 0.0008

<sup>a</sup> Sample calculation results using VIM provided by Roger N. Blomquist, Argonne National Laboratory.

Table 14.b. Sample Calculation Results (United Kingdom).

Code (Cross Section Set→ Case. #↓	MONK 8A (JEF2.2) <sup>(a)</sup>	MONK 8A (ENDF/B-VI.3) <sup>(a)</sup>
1	1.0076 ± 0.0005	0.9987 ± 0.0005
2	1.0107 ± 0.0005	1.0013 ± 0.0005

<sup>a</sup> Sample calculation results using MONK 8A provided by Roger N. Blomquist, Argonne National Laboratory.

## 5.0 REFERENCES

1. J. K. Fox, L. W. Gilley, and E. R. Rohrer, "Critical Mass Studies, Part VIII Aqueous Solutions of U233," Neutron Physics Division, ORNL-2143, Oak Ridge National Laboratory, 1959.

## APPENDIX A: TYPICAL INPUT LISTINGS

### A.1 KENO Input Listings: CSAS25 with SCALE 27-Group ENDF/B-IV Cross Sections

The following are KENO V.a input files for the use of the CSAS25 sequence and the SCALE 27-group cross sections. SCALE Version 4.4a was used for these calculations. The data showing average  $k_{\text{eff}}$  for a particular number of generations skipped was examined, and the  $k_{\text{eff}}$  for the number of generations skipped that gave the lowest standard deviation was reported in Section 4. (This is the value from the KENO V.a output just before the plot of average  $k_{\text{eff}}$  by generation skipped.) The sample calculations used 200 active generations of 1000 neutrons per generation, after skipping 3 initial generations.

```
=csas25
U233-SOL-THERM-005, Case 1
27gr infh
u-233      1 0 1.6011E-04  293. end
u-234      1 0 7.4332E-07  293. end
u-238      1 0 1.3981E-06  293. end
h          1 0 6.5028E-02  293. end
o          1 0 3.4077E-02  293. end
n          1 0 4.3047E-04  293. end
al         2 0 5.9881E-02  293. end
si         2 0 5.8108E-04  293. end
h          3 0 6.6735E-02  293. end
o          3 0 3.3368E-02  293. end
end comp
exp 37 simplified model
read geometry
unit 1
sphere 1 1 13.2118
sphere 2 1 13.3409
sphere 3 1 28.5809
end geometry
end data
end
```



U233-SOL-THERM-005

```
=csas25
U233-SOL-THERM-005, Case 2
27gr infh
u-233      1 0 1.2707E-04  293. end
u-234      1 0 5.8994E-07  293. end
u-238      1 0 1.1096E-06  293. end
h          1 0 6.5403E-02  293. end
o          1 0 3.3942E-02  293. end
n          1 0 3.4152E-04  293. end
al         2 0 5.9881E-02  293. end
si         2 0 5.8108E-04  293. end
h          3 0 6.6735E-02  293. end
o          3 0 3.3368E-02  293. end
end comp
exp 39 simplified model
read geometry
unit 1
cyli      1 1  12.7287  25.5      -0.1482
cyli      2 1  12.8578  25.6291  -0.2773
cyli      3 2  28.0978  40.8691 -15.5173
end geometry
end data
end
```

## **A.2 KENO Input Listings: CSAS25 with SCALE 238-Group ENDF/B-V Cross Sections**

The following are KENO V.a input files for the use of the CSAS25 sequence and the SCALE 238-group cross sections. SCALE Version 4.4a was used for these calculations. The data showing average  $k_{\text{eff}}$  for a particular number of generations skipped was examined, and the  $k_{\text{eff}}$  for the number of generations skipped that gave the lowest standard deviation was reported in Section 4. (This is the value from the KENO V.a output just before the plot of average  $k_{\text{eff}}$  by generation skipped.) The sample calculations used 200 active generations of 1000 neutrons per generation, after skipping 3 initial generations.

```
=csas25
U233-SOL-THERM-005, Case 1
238gr infh
u-233      1 0 1.6011E-04  293. end
u-234      1 0 7.4332E-07  293. end
u-238      1 0 1.3981E-06  293. end
h          1 0 6.5028E-02  293. end
o          1 0 3.4077E-02  293. end
n          1 0 4.3047E-04  293. end
al         2 0 5.9881E-02  293. end
si         2 0 5.8108E-04  293. end
h          3 0 6.6735E-02  293. end
o          3 0 3.3368E-02  293. end
end comp
exp 37 simplified model
read geometry
unit 1
sphere 1 1 13.2118
sphere 2 1 13.3409
sphere 3 1 28.5809
end geometry
end data
end
```

U233-SOL-THERM-005

```
=csas25
U233-SOL-THERM-005, Case 2
238gr infh
u-233      1 0 1.2707E-04  293. end
u-234      1 0 5.8994E-07  293. end
u-238      1 0 1.1096E-06  293. end
h          1 0 6.5403E-02  293. end
o          1 0 3.3942E-02  293. end
n          1 0 3.4152E-04  293. end
al         2 0 5.9881E-02  293. end
si         2 0 5.8108E-04  293. end
h          3 0 6.6735E-02  293. end
o          3 0 3.3368E-02  293. end
end comp
exp 39 simplified model
read geometry
unit 1
cyli      1 1  12.7287  25.5      -0.1482
cyli      2 1  12.8578  25.6291  -0.2773
cyli      3 2  28.0978  40.8691 -15.5173
end geometry
end data
end
```

### A.3 MCNP Input Listings

The following are MCNP input files for utilizing continuous-energy ENDF/B-V.0 cross sections. MCNP4C was used for these calculations. The value of  $k_{\text{eff}}$  reported in Section 4 is the final estimated combined collision/absorption/track-length  $k_{\text{eff}}$  given in the MCNP output. The sample calculations used 200 active generations of 1500 neutrons per generation, after skipping 50 initial generations.

U233-SOL-THERM-005, Case 1

C Cell Cards with material densities

```
1 1 0.099698 -1      imp:n=1
2 2 0.060462 -2 1    imp:n=1
3 3 0.100103 -3 2    imp:n=1
4 0          3      imp:n=0
```

C Surface cards

```
1 SO 13.2118
2 SO 13.3409
3 SO 28.5809
```

C Data Cards

```
M1 1001.50c 6.5028e-2 8016.50c 3.4077e-2 7014.50c 4.3047e-4
    92233.50c 1.6011e-4 92234.50c 7.4332e-7 92238.50c 1.3981e-6
MT1 lwtr.01t
C Al-2S
M2 13027.50c 0.059881 14000.50c 5.8108e-4
c Water reflector
M3 8016.50c 0.033368 1001.50c 0.066735
MT3 lwtr.01t
kcode 1500 1.0 50 250 7000
ksrc 0.0 0.0 0.0
```

NEA/NSC/DOC/(95)03/V  
Volume V

U233-SOL-THERM-005

U233-SOL-THERM-005, Case 2

C Cell Cards with material densities

1 1 0.099815 -1 6 -7 imp:n=1  
2 2 0.060462 (1:7:-6)(-2 5 -8) imp:n=1  
3 3 0.100103 (2:8:-5)(-3 4 -9) imp:n=1  
4 0 3:-4: 9 imp:n=0

C Surface cards

1 CX 12.7287  
2 CX 12.8578  
3 CX 28.0978  
4 PX -15.5173  
5 PX -0.2773  
6 PX -0.1482  
7 PX 25.5  
8 PX 25.6291  
9 PX 40.8691

C Data Cards

M1 1001.50c 6.5403e-2 8016.50c 3.3942e-2 7014.50c 3.4152e-4  
92233.50c 1.2707e-4 92234.50c 5.8994e-7 92238.50c 1.1096e-6

MT1 lwtr.01t

C Al-2S

M2 13027.50c 0.059881 14000.50c 5.8108e-4

c Water reflector

M3 8016.50c 0.033368 1001.50c 0.066735

MT3 lwtr.01t

kcode 1500 1.0 50 250 7000

ksrc 12.0 0.0 0.0

#### **A.4 VIM Input Listing**

VIM 4.0 was run for 105 generations with 10000 neutrons per generation. The first five generations were skipped before averaging, so each computed VIM result is the average of 1,000,000 neutron histories. Continuous energy ENDF/B-V and ENDF/B-VI cross sections were used for the VIM calculations. Hydrogen with a water thermal kernel was used for the solution and reflector.

U233-SOL-THERM-005

VIM Input Listing for Case 1 of Table 14.a.

```

1111192347      U233-SOL-THERM-005 Case 1      01
  100    3    0  005    0    0      02
10000 10000    1    1    0      03
    1    1    0    0   50    0      04
    8    3    3    1    4 10000      05
9999999900.0    1.0-5    275.0    1.0    1.0-5    1.4191+7    6an
    0.90    1.00    0.0    0.0      6bn

40300 60300100300240300260300380300420300900300      08
                                                    09
                                                    10
    0    0    4      20
SPH    1  0.000000    0.0000    0.0  13.2118      21
SPH    2  0.000000    0.0000    0.0  13.3409      21
SPH    3  0.000000    0.0000    0.0  28.5809      21
RPP    4 -13.0    13.0    -13.0  13.0    -13.0    13.0      21
END                                                    21
U233    6    1      22
IVES    6    2   -1      22
REFL    6    3   -2      22
LEAK    6   -3      22
END                                                    22
                                                    23
    1  101  1          2  200  2          3  300  3      24
    4  000 -1      24
40300 60300100300260300420300900300      45 c1 solution
240300380300      45 c2 S3 A1
260300900300      45 c2 water
  1.3981e-06  7.4332e-07  1.6011e-04  3.4077e-02  4.3047e-04  6.5028e-02      46 c1 solution
  5.9881e-02  5.8108e-04      46 c2 S3 A1
  3.3368e-02  6.6735e-02      46 c3 water
    1.0000-5      50

```

U233-SOL-THERM-005

VIM Input Listing for Case 2 of Table 14.a.

```
1111192347      U233-SOL-THERM-005 Case 2      01
  100    3    0  005    0    0      02
10000 10000    1    1    0      03
    1    1    0    0   50    0      04
    8    3    3    1    4 10000      05
9999999900.0    1.0-5    275.0    1.0    1.0-5    1.4191+7    6an
    0.90    1.00    0.0    0.0      6bn

40300 60300100300240300260300380300420300900300      08
                                                    09
                                                    10
    0    0    4      20
CYL  1  0.000000    0.0000 -12.8241  25.6482  12.7287      21
CYL  2  0.000000    0.0000 -12.9532  25.9064  12.8578      21
CYL  3  0.000000    0.0000 -28.1932  56.3864  28.0978      21
RPP  4 -13.0    13.0    -13.0  13.0    -13.0    13.0      21
END                                                    21
U233  6    1      22
IVES  6    2   -1      22
REFL  6    3   -2      22
LEAK  6   -3      22
END                                                    22
                                                    23
    1  101  1          2  200  2          3  300  3      24
    4  000 -1      24
40300 60300100300260300420300900300      45 c1 solution
240300380300      45 c2 S3 A1
260300900300      45 c2 water
  1.1096e-06  5.8994e-07  1.2707e-04  3.3942e-02  3.4152e-04  6.5403e-02      46 c1 solution
  5.9881e-02  5.8108e-04      46 c2 S3 A1
  3.3368e-02  6.6735e-02      46 c3 water
    1.0000-590|      50
```



## **A.5 MONK Input Listings**

MONK 8A was run with four settling stages to converge the initial source followed by 231 stages to accumulate histories. There were 2000 starters per stage, and 10 generations per stage. The JEF 2.2 and ENDF/B-VI cross section libraries with 13193 energy groups were used for the MONK 8A calculations. Hydrogen with a water thermal kernel was used for the solution and the reflector.

MONK Input Listing for Case 1 of Table 14.b.

\* NOLIST

COLUMNS 1 132

\* NEA/NSC U233-SOL-THERM-005 Case 1 JEF2.2

BEGIN MATERIAL SPECIFICATION

NMATERIALS 3

\* material 1 - core

\* material 2 - central h2o

ATOMS

MATERIAL 1 DENSITY 0.0

U233 PROP 1.6011e-04

U234 PROP 7.4332e-07

U238 PROP 1.3981e-06

O16 PROP 3.4077e-02

N14 PROP 4.3047e-04

H1INH2O PROP 6.5028e-02

ATOMS

MATERIAL 2 DENSITY 0.0

AL PROP 5.9881e-02

SI PROP 5.8108e-08

ATOMS

MATERIAL 3 DENSITY 0.0

O16 PROP 3.3368e-02

H1INH2O PROP 6.6735e-02

\* USE J2HINH2O FOR H1 IN ALL MATERIALS

\* USE E6HH2O FOR H1 IN ALL MATERIALS

END

BEGIN CONTROL DATA

\* STAGES 0 200 0200 STDV 0.0050

STAGES -3 800 2000 STDV 0.0005

SUPERHIST 10 1.0

END

BEGIN MATERIAL GEOMETRY

PART 1 NEST

SPHERE M1 0.0 0.0 0.0 13.2118

SPHERE M2 0.0 0.0 0.0 13.3409

U233-SOL-THERM-005

SPHERE M3 0.0 0.0 0.0 28.5809

SPHERE M0 0.0 0.0 0.0 40.

\* ALBEDO 0 1 1 0 1 1

END

BEGIN SOURCE GEOMETRY

ZONEMAT

ALL /

END

BEGIN ACTION TALLIES

MATACT

\* NO ACTION TALLIES

END

U233-SOL-THERM-005

MONK Input Listing for Case of Table 14.b.

\* NOLIST

COLUMNS 1 132

\* NEA/NSC U233-SOL-THERM-005 Case 2 JEF2.2

BEGIN MATERIAL SPECIFICATION

NMATERIALS 3

\* material 1 - core

\* material 2 - AlSi can

\* material 3 - h2o

ATOMS

MATERIAL 1 DENSITY 0.0

U233 PROP 1.2707e-04

U234 PROP 5.8994e-07

U238 PROP 1.1096e-06

O16 PROP 3.3942e-02

N14 PROP 3.4152e-04

H1INH2O PROP 6.5403e-02

ATOMS

MATERIAL 2 DENSITY 0.0

AL PROP 5.9881e-02

SI PROP 5.8108e-08

ATOMS

MATERIAL 3 DENSITY 0.0

O16 PROP 3.3368e-02

H1INH2O PROP 6.6735e-02

\* USE J2HINH2O FOR H1 IN ALL MATERIALS

\* USE E6HH2O FOR H1 IN ALL MATERIALS

END

BEGIN CONTROL DATA

\* STAGES 0 200 0200 STDV 0.0050

STAGES -3 800 2000 STDV 0.0005

SUPERHIST 10 1.0

END

BEGIN MATERIAL GEOMETRY

PART 1 NEST

ZROD M1 0.0 0.0 -12.8241 12.7287 25.6482

U233-SOL-THERM-005

ZROD M2 0.0 0.0 -12.9532 12.8578 25.9064

ZROD M3 0.0 0.0 -28.1932 28.0978 56.3864

ZROD M0 0.0 0.0 -30.0 30. 60.0

\* ALBEDO 0 1 1 0 1 1

END

BEGIN SOURCE GEOMETRY

ZONEMAT

ALL /

END

BEGIN ACTION TALLIES

MATACT

\* NO ACTION TALLIES

END

## APPENDIX B: SOLUTION HEIGHT DETERMINATION

According to E. R. Rohrer,<sup>a</sup> the height of the solution in the manifold was calibrated using a clear flexible hose connection and a meter stick. A point was then chosen on the wall and another on the manifold at which the height of solution in the vessel was zero. At that point the vessel was empty of fissile solution. As the manifold was raised, its liquid level dropped, the reaction vessel filled in proportion to the respective areas of the two, i.e., the smaller the diameter of the reaction vessel, the smaller the fall would be in the manifold liquid height as the position of the manifold on the wall was adjusted. At equilibrium, of course, the heights in the manifold and the reaction vessel would be equal.

The change in height of the fissile solution in the vessel was determined using the following relationship:

$$\Delta H = \frac{MA_m}{A_v + A_m}$$

where  $M$  is the initial movement in units of length of the manifold,  $A_v$  is the area of the vessel,  $A_m$  is the area of the manifold, and  $\Delta H$  is the final change in height of both the manifold solution and vessel solution since the two changes are equal. The final height, it will be observed, must be a value between 0 and the manifold height. Proper calibration of the manifold was also necessary to determine its cross-sectional area for use in this formula.

According to Rohrer, bubbles were not a problem; however, in a few cases with concentrated uranium solutions, plugs did occur and then the level of solution reached equilibrium very slowly if at all. Whenever changes were made in the total solution volume in the vessels, such as would occur when the solution was diluted or renewed, the manifold zero point would shift.

---

<sup>a</sup>E. R. Rohrer, personal communication to J. T. Shor, Oak Ridge National Laboratory, July 1997.